



CVD-HNet: Classifying Pneumonia and COVID-19 in Chest X-ray Images Using Deep Network

S. Suganyadevi¹ · V. Seethalakshmi¹

Accepted: 29 May 2022 / Published online: 19 June 2022

© The Author(s), under exclusive licence to Springer Science+Business Media, LLC, part of Springer Nature 2022

Abstract

The use of computer-assisted analysis to improve image interpretation has been a long-standing challenge in the medical imaging industry. In terms of image comprehension, Continuous advances in AI (Artificial Intelligence), predominantly in DL (Deep Learning) techniques, are supporting in the classification, Detection, and quantification of anomalies in medical images. DL techniques are the most rapidly evolving branch of AI, and it's recently been successfully pragmatic in a variety of fields, including medicine. This paper provides a classification method for COVID 19 infected X-ray images based on new novel deep CNN model. For COVID19 specified pneumonia analysis, two new customized CNN architectures, CVD-HNet1 (COVID-HybridNetwork1) and CVD-HNet2 (COVID-HybridNetwork2), have been designed. The suggested method utilizes operations based on boundaries and regions, as well as convolution processes, in a systematic manner. In comparison to existing CNNs, the suggested classification method achieves excellent Accuracy 98 percent, F Score 0.99 and MCC 0.97. These results indicate impressive classification accuracy on a limited dataset, with more training examples, much better results can be achieved. Overall, our CVD-HNet model could be a useful tool for radiologists in diagnosing and detecting COVID 19 instances early.

Keywords Deep learning · COVID 19 · CNN · X-ray · Accuracy · Matthews correlation coefficient

1 Introduction

With the rapid advancement of artificial intelligence, an increasing number of researchers are focusing on intelligence, deep learning-based diagnostic approaches. A few of them have produced some very impressive outcomes. DL (Deep Learning) techniques are the significant contributor to the current emergence of AI in practically every aspect of life [1].

✉ S. Suganyadevi
suganya3223@gmail.com

V. Seethalakshmi
seethav@kpri.ac.in

¹ Department of Electronics and Communication Engineering, KPR Institute of Engineering and Technology, Coimbatore, Tamilnadu 641 407, India

It's a direct result of current achievements in a wide range of scientific domains, including chemical structure analysis, Particle Physics, Computer Vision, Natural Language Processing, DNA analysis, brain circuit's studies. It has recently stimulated the importance of clinical imaging investigators, indicating which it holds enormous promise for the field's future [2]. The Deep Learning model enables machines that can learn extremely complicated data representational mathematical models, which can then be utilised to do precise data analysis [3]. These methods perform linear functions and/or non-linear of the input image or data which are weighted with the model parameters in a hierarchical fashion [4]. Deep learning approaches have a common aim of continuously learning the features of a computer model using training datasets, so that the model improves over time at performing a specified task, such as classification and detection, over that datasets under a stated metrics [5].

Machine Learning has been employed in the medical imaging sector since the 1960s. However, it was in the 1990s that the first major contributions relating to contemporary Deep Learning techniques appeared in the Medical Imaging field [6]. In recent decades, medical imaging modalities including X-ray, Magnetic Resonance (MR), Mammography, Computed Tomography (CT), Positron Emission Tomography (PET) and ultrasound had grown more significant in early disease detection, diagnosis, and treatment. Today's Medical imaging techniques including MRI/fMRI, X-ray, CT, and PET scanners provide a plethora of complicated and highly useful images to computer-aided diagnosis (CAD) [6, 7].

Appropriate feature extraction [8] or feature illustration is at the core of machine learning's attainment in completing specified jobs. Relevant features were traditionally defined by medical specialists depending on their understanding of the aim of the field, making it difficult for non-experts [9] to use machine learning models for their own research. Deep learning models, on the other hand, has overcome these challenges by integrating the feature engineering process into a learning phase. That example, inspite of manually extracting features, DL techniques just necessitates a collection of image data's and some basic pre-processing [10].

The current technological improvements have resulted in the combination of DL classifiers and medical images providing greater impressive outcomes comparable to conventional RT-PCR screening while increasing the accuracy of COVID 19 case prediction and diagnosis. From December 2019, a novel coronavirus (SARS-CoV-2) had spread across Wuhan to the rest areas of China and numerous other nations. And over 230 million cases have been confirmed, with approximately 5 million deaths had been recorded worldwide by October 1 2021. (<https://www.worldometers.info/coronavirus>). Figure 1 shows the Global Situation of COVID-19 Total Cases, Total Deaths and Recovered Cases taken by World meter. Which has far implications on people's daily lives, global economy and public health. It's critical to identify confirmed cases as quickly as possible to stop the outbreak from growing faster and to help patients as quickly as possible [11]. The demand of supplemental diagnostic equipment has grown since there are no effective automated tool-kits available. Such images convey essential information regarding the COVID-19 virus, as according latest researches obtained employing radiological imaging techniques. Improved AI based techniques paired with imaging techniques can help to detect exact disease, along with solve the issue of a physician scarcity in rural regions [12].

One among the most vital significant drawbacks of chest x-ray analysis is their being unable to recognise COVID-19 in its early phases due to a lack of sensitivity while performing GGO detection [13–15]. Deep learning models that have been well-trained, on the other hand, can concentrate on details which the human eye misses, potentially reversing this view.

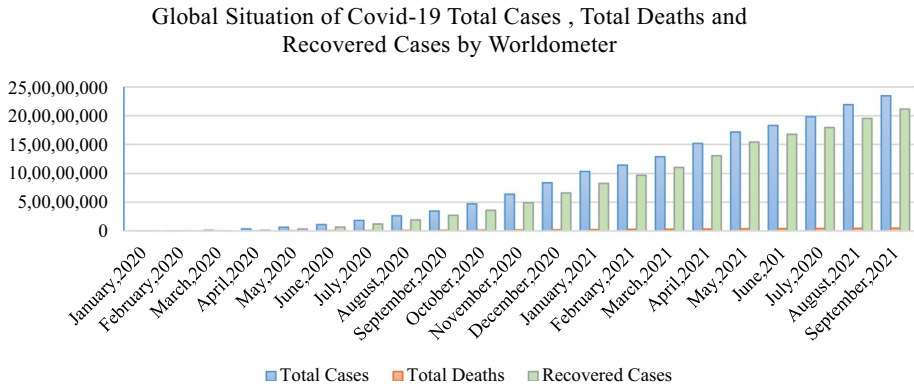


Fig. 1 Global Situation of COVID-19 Total Cases, Total Deaths and Recovered Cases by Worldometer

In Sect. 2 we present some general classifications of learnings, In Sect. 3 we cover the principles of extracting high-level representations from data using neural networks and deep architectures such as Artificial Neural Network (ANN), Recurrent Neural Network (RNN) and Convolutional Neural Network (CNN) [11]. Section 4 covers classification approach based on Proposed COVID-HNet (COVID-HYBRIDNet). Finally, in Sect. 5, we summarise the study patterns of one of application of deep learning such as COVID19 classification and finally in Sect. 6 we present conclusions and make some recommendations for future improvements.

2 Learning Types

The following are the 14 categories of learning that we must be acquainted with as AI specialists. Figure 2 shows the various kinds of learnings available in machine learning.

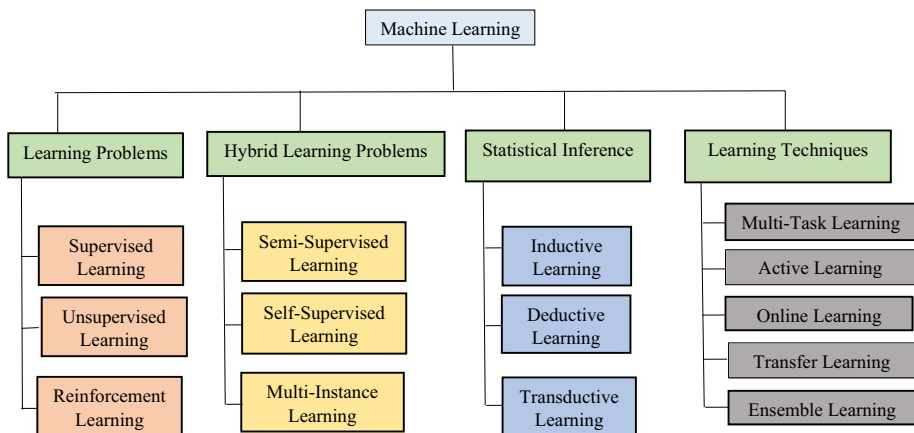


Fig.2 Learning Types

2.1 Supervised Learning

Supervised learning is among the most prevalent types of Machine Learning (ML). In this instance, the algorithm is given training on annotated data. In spite of the fact that appropriate annotated data is mandatory used for this method to work, this kind of learning can be extremely effective while utilised under the right situations [12–14].

The environment has a set of data inputs and resulting data outputs $(x_t, y_t) \sim p$ when contemplating such a technique. If the input is x_t , the smart agent will assume $y_{t^A} = f(x_t)$ and return (y_{t^A}, y_t) as a loss value [15]. In this classification scenario, normally y would be a class value which is always scalar but it could be a vector of continuous data in a regression setting [16].

Deep Neural Networks (DNNs), Recurrent Neural Networks (RNNs) and Convolutional Neural Networks (CNNs) are examples of supervised learning techniques for DL. Long Short-Term Memory (LSTM) and Gated Recurrent Units (GRUs) techniques are also included in the RNN category [17]. The primary benefit of this technology is the capacity to gather data or develop a data output using prior knowledge. The downside of this strategy is that when the training set lacks samples that should be in a class, the decision boundary may be overstrained. In general, this strategy is easier to learn than other high-performance learning techniques [18].

2.2 Unsupervised Learning

Unsupervised learning algorithms are trained to discover patterns in unlabelled data, such as latent subspaces. Conventional unsupervised methods includes Principal Component Analysis (PCA) and clustering approaches. This implies that no human labour is necessary to make the dataset machine-readable, enabling the programme to work on much larger datasets [19].

When compared to supervised learning, unsupervised learning algorithms allow users to complete more complicated processing tasks. However, when compared to other natural learning methods, unsupervised learning is more unpredictable [20]. Clustering, anomaly detection, and neural networks are examples of unsupervised learning methods [21].

Some of the most newly invented elements of the DL category, such as Deep Boltzmann Machines, Auto-Encoders, and Generative adversarial Network, have fared well along nonlinear dimensionality reduction (DR) and clustering issues [22]. RNNs including LSTM and GRUs approaches, have now been employed used in a variety of applications for unsupervised learning. Unsupervised learning's key drawbacks are its inability to give precise data sorting information and its computational complexity. Clustering is one of the most often used unsupervised learning techniques [23].

2.3 Reinforcement Learning

Reinforcement Learning (RL) is based on interacting with the environment, whereas supervised learning is based on a set of data that is presented. This method was created in 2013 with the help of Google Deep Mind. As a result, numerous improved reinforcement learning approaches have been developed [24].

Reinforcement learning is a machine learning training strategy that involves rewarding specific behaviours while punishing unwanted ones [25]. A reinforcement learning

agent can observe and comprehend its surroundings, execute actions, and learn through trial and error in general. There is no answer in reinforcement learning, but the reinforcement agent decides how to complete the job. It is obligated to learn from its experience in the absence of a training dataset.

Since the reinforcement learning technique does not have a straightforward loss function, it is far more difficult to perform than typical supervised techniques [25, 26]. Furthermore, There have been two key differences among supervised and reinforcement learning. first, there is no comprehensive availability towards the function, necessitating optimization, suggesting that it should be questioned such as through interaction, and second, the state has been interacted with is based on a surroundings, with the data relying on previous actions [27].

3 Deep Models

Hinton and Salakhutdinov released an article in the science journal in 2006 that ushered in the DL era [28]. They demonstrated that a neural network with hidden layers was crucial in boosting learning's features' power [29].The accuracy of these algorithms can be improved while classifying different types of data [30]. Figure 3 describes the general classification of machine learning model [31].

3.1 Artificial Neural Network (ANN)

A single perceptron or neuron could be thought of a Regression Model. At each layer of an ANN, there are numerous perceptron's/neurons [31]. Because data inputs are exclusively processed in the forward direction, that ANN is furthermore known as a Feed-Forward Neural Network. ANN comprises of 3 layers explicitly Input, Hidden and Output layer

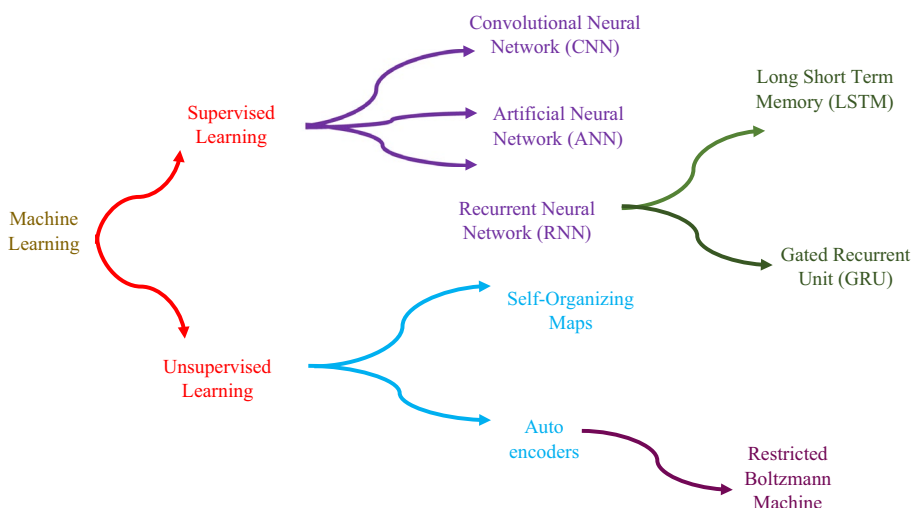


Fig.3 General Classification of Machine Learning

[32]. The data is received by the input layer, evaluated by the hidden layer, and synthesized by the output layer. In essence, each layer is attempting to learn specific weights [33].

3.1.1 Advantages

Artificial Neural Network learns any non—linear function. As a result, these networks are commonly referred to as Universal Function Approximators [34]. An artificial neural network (ANN) can train weights that map every input to the desired output. One of its primary reasons for universal approximation would be the activation function [35]. Activation functions are used to establish the network’s non-linear properties. This makes it easier for the network to learn any complicated input–output connection [36].

3.1.2 Challenges

Before training an ANN model in solving picture classification challenge would be to transform a two-dimensional picture into a one-dimensional vector [37]. This has some disadvantages, as the image size grows larger, the number of trainable parameters grows dramatically. The spatial properties of an image are lost while using ANN. Spatial characteristics pertain to how pixels are arranged in an image [38].

In most of these Neural Network models, the Vanishing and Exploding Gradient will be a frequent problem. Back propagation algorithm is also linked with this issue [39]. This Back propagation algorithm finds the gradients and updates the weights of a neural network. As a result, when a highly deep neural network (DNN) propagates backward, the gradient vanishes and bursts, resulting in vanishing and exploding gradients [40]. ANN does not capture sequence information in the data input, which is required for handling with sequence data sets [41].

3.2 Recurrent Neural Network (RNN)

Recurrent Neural Networks are used to address problems involving time series data, text data, and audio data. RNNs were originally designed for the analysis of discrete sequence of data [42]. It will be seen of a generalisation of Multilayer perceptron since both input, output could be of various lengths, making them appropriate for applications like machine translation, where the input and output are a phrase from the source and target languages, respectively [43]. The model learns a distribution across classes $P(y|x_1, x_2, \dots, x_T)$ from a series x_1, x_2, \dots, x_T instead of only one vector x in a classification context [44].

At time t , the basic RNN keeps a hidden or latent state h , which is the result of a nonlinear mapping between its prior state h_{t-1} and input $x(t)$. Here R and W are weight matrices shared among time shown in Eq. (1) [45].

$$\sigma(Wx_t + Rh_{t-1} + b) = h_t \quad (1)$$

3.2.1 Advantages

During making predictions, RNN preserves the sequence data available in the input datasets, which is the dependent seen among words in the text [45]. The parameters of RNNs

are shared between time steps. This is commonly referred to as parameter sharing. As a result, there are lesser factors to train and the computing cost is lower [46].

3.2.2 Challenges

The vanishing and exploding gradient issue is a prevalent issue in all forms of Neural Networks, and it also affects deep RNNs that is RNNs with higher number of time steps [47].

3.3 Convolutional Neural Network (CNN)

In DL community, Convolutional Neural Networks (CNN) are all the rage right now [48]. These CNN models are employed in a variety of regions and applications, but they are particularly common in picture and video dealing out projects [49]. Filters, often known as kernels, are the building components of CNNs. The kernels are utilised to extract relevant information from input by using convolution approach. Even though CNNs had been developed to handle issues with image data, they can function well with sequential inputs [50]. The inputs to SAE, DBN, and DBM deep models are always in vector form. However, structural data among surrounding pixels is a significant source of data for medical pictures [51]. As a result, image vectorization invariably eliminates structural and configurable information. A CNN is meant to best utilize spatial and setup information by taking 2-dimensional and 3-dimensional images as input [52]. In the structure of a CNN, convolutional layers are alternated with pooling levels, preceded by fully connected layers, as in a traditional multilayer neural network. The working model of the basic structure for a CNN is shown in Fig. 4 [53].

3.3.1 Advantages

CNN automatically learns the filters without revealing them. These filters aid in the extraction of the most relevant and appropriate features from the incoming data [54]. The spatial features of a picture is acquired by CNN. The pattern of pixels and their interrelation in an image are referred to as spatial characteristics [55]. They assist us in precisely identifying an object, as well as its location and relationship to other things in a picture. The concept

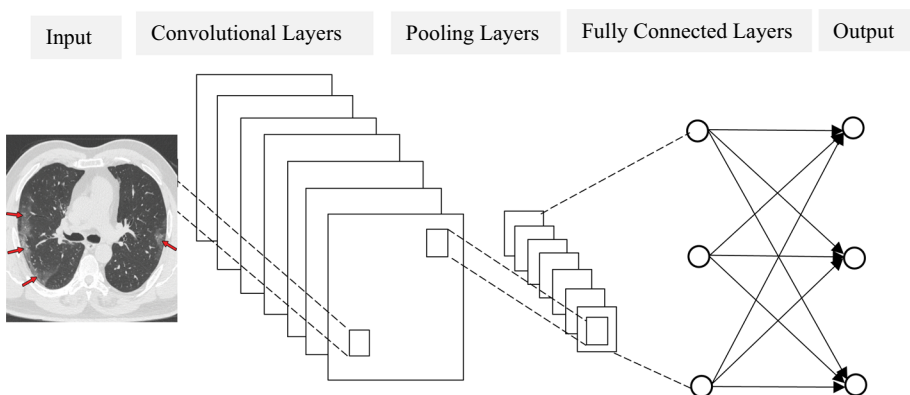


Fig. 4 General Architecture of CNN

of parameter sharing is also used by CNN. A feature map is created by applying a single filter to various portions of an input [56].

3.3.2 Challenges

After a sample of data has been preprocessed, backprop is a way for determining the influence of each weight in the error, and most good optimization algorithms like SGD, ADAM, etc. uses to find the gradients [57]. Back propagation has performed admirably in recent years, but it is not an effective method of learning because it necessitates a large dataset [58].

When we talk about translational invariance, we mean that if an object's orientation or position changes significantly, the neuron that is meant to detect that object may not fire [59]. The problem is partially solved through data augmentation, but it is not completely solved [60].

Pooling layers is a huge mistake since it loses a lot of useful information and ignores the relationship between the parts and the whole [61]. For example, if we're talking about a face detector, we need to combine various traits (mouth, two eyes, a face oval, and a nose) to declare it's a face. Table 1 provides a comparison between ANN, RNN and CNN [62]. Various Processes involved in CNN model is shown in Fig. 5.

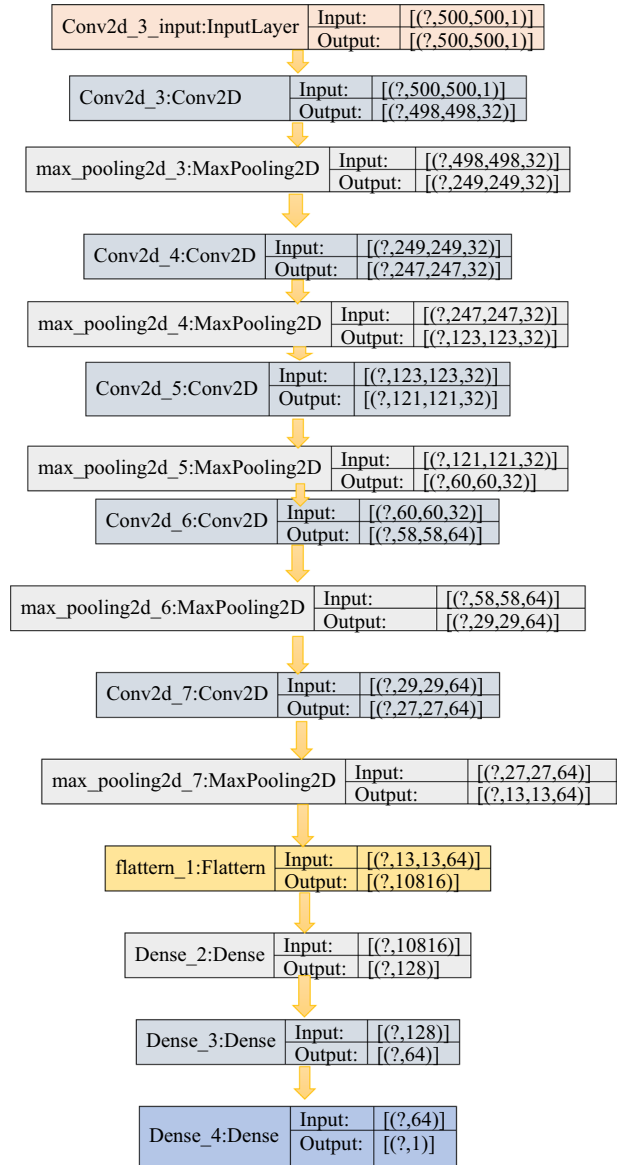
4 Deep CVD-HNet Architecture and Classification

We used a new novel deep CNN models to identify the clear COVID 19 Pneumonia abnormalities in chest X-ray images in this work. Because of their high capacity for learning prominent features and patterns revealed by images, deep CNN models have been widely used in image recognition and classification. CNNs are employed for both feature creation and classification because of their high learning capabilities. We termed CVD-HNet1 (COVID-HybridNet1) and CVD-HNet2 (COVID-HybridNet2) are two new Convolutional Neural network designs depends on boundaries and regions based procedures for COVID 19 specialized pneumonia in X-ray samples. These approaches are tuned from beginning to end to acquire pneumonia-specialized data from X-ray pictures. The recommended deep CNN designs use fully—connected layers for categorization [63]. The subsequent subsections summarise the design features.

Table 1 Comparison between ANN, RNN and CNN

	ANN	RNN	CNN
Data (Input)	Tabular data	Sequence data (i) Time Series (ii) Text (iii) Audio	Image data
Recurrent Connections	Not Available	Available	Not Available
Parameter sharing	No	Yes	Yes
Spatial relationship	No	No	Yes
Vanishing & exploding gradient	Yes	Yes	Yes

Fig.5 Process of the CNN model



The suggested CVD-HNets design is inspired by traditional image processing methods [64] and also is built on the concept of leveraging fundamental features in images. In order to efficiently learn the COVID 19 unique patterns of pneumonia, we rigorously synergized the usage of boundaries and regions based procedures, along with convolutional processes in CNN to evaluate the advantages of this suggested boundaries and region based approach in information extraction with CNN models, we employed VGG 16 and ResNet 18 as baseline methods [65, 66]. In this study, we gathered 7000 pictures from the Open Source GitHub and Kaggle repositories, which included 3500 COVID 19 patients and 3500 healthy people. VGG 16 can

be a state-of-the-art CNN that uses mean pooling throughout design to regulate picture size and convolution operations for feature extraction. Rather than pooling, ResNet 18 employs strided convolution for picture down sampling, taking benefit of convolution in tandem with the Relu activation function enabling feature extraction. Four convolution blocks make up the proposed CVD-HNet1. Batch normalisation, a convolutional layer (Eq. (2)) and also ReLU as an activation function are all included in every block. After each convolutional block, average (Eq. (3)) and max pooling (Eq. (4)) are used to perform boundaries and regions based procedures. These methods improve the image’s region-specific qualities and boundaries data, whilst the convolutional process extracts the image’s sequence features. The proposed model employs fully—connected layers, as shown in Eq. (5), to produce goal information for classification. The setup of the proposed CVD-HNet architecture for the COVID 19 dataset is summarised in Fig. 6.

$$f_{x,y} = \sum_{a=1}^p \sum_{b=1}^q f_{x+a-1,y+b-1} K_{a,b} \tag{2}$$

$$f_{x,y}^{avg} = \frac{1}{W} \sum_{a=1}^w \sum_{b=1}^w f_{x+a-1,y+b-1} \tag{3}$$

$$f_{x,y}^{max} = \max_{a=1,\dots,w,b=1,\dots,w} f_{x+a-1,y+b-1} \tag{4}$$

Layer (type)	Output Shape	Param #
conv2d (Conv2D)	(None, 150, 150, 16)	448
max_pooling2d (MaxPooling2D)	(None, 75, 75, 16)	0
dropout (Dropout)	(None, 75, 75, 16)	0
conv2d_1 (Conv2D)	(None, 75, 75, 32)	4640
max_pooling2d_1 (MaxPooling2D)	(None, 37, 37, 32)	0
conv2d_2 (Conv2D)	(None, 37, 37, 64)	18496
max_pooling2d_2 (MaxPooling2D)	(None, 18, 18, 64)	0
dropout_1 (Dropout)	(None, 18, 18, 64)	0
flatten (Flatten)	(None, 20736)	0
dense (Dense)	(None, 512)	10617344
dense_1 (Dense)	(None, 1)	513
Total params: 10,641,441		
Trainable params: 10,641,441		
Non-trainable params: 0		

Fig. 6 Model Summary and Training Parameters of CVD-HNet Architecture

Table 2 Comparison among CVD-HNets in contrast to baseline methods

Deep models	Accuracy	F score	MCC	Depth
VGG16	96.16	0.98	0.95	18
Resnet18	96.21	0.98	0.96	16
CVD-HNet1	97.46	0.99	0.97	10
CVD-HNet2	97.75	0.99	0.97	08

Table 3 ADAM based Learning capability assessment using baseline approaches and proposed CVD-HNets

Deep Models	Accuracy	Sensitivity	Specificity	TP	FP	FN	TN	MCC	F Score
VGG16	95.90	0.96	0.96	639	26	28	625	0.95	0.96
Resnet18	96.64	0.97	0.97	641	21	23	628	0.96	0.97
CVD-HNet1	98.09	0.98	0.98	651	12	13	636	0.97	0.99
CVD-HNet2	98.84	0.99	0.99	660	8	7	628	0.98	0.99

$$v = \sum_d^D \sum_c^C u_{dfc} \quad (5)$$

The regions operator helps to smooth out region variances through average pooling (Eq. (3)), and so functions as a noise suppression for X-ray imaging aberrations. The edge operators, on the other hand, uses the max pooling operation to promote CNN to acquire effective feature and narrow features (Eq. (4)). To limit the possibilities of overfitting, drop-out is given to the fully-connected layers. CVD-HNet-2, on the other hand, is built on the same concept but with more depth.

COVID-HNet-2 is made by 4 convolutional blocks and each with distinct no. of operations. Table 2 provides the performance comparison of suggested CVD-HNETs and Existing CNNs. By features extraction from the proposed COVID-penultimate HNet's layer and assigning it to the ADAM classifier, the suggested COVID-mapping HNet's capability is tested and it's shown in Table 3.

4.1 Implementation of Existing Standard CNNs

VGG, Inception, GoogleNet, ResNet, SqueezeNet, Xception and DenseNet [67–75] were used to compare several existing state-of-the-art deep CNN algorithms. These CNNs were employed extensively for a broad range of picture classification issues, including COVID 19 X-ray classification by numerous studies. These methods differ in blocks architecture and design, but they all used a unique unit of pooling process for complexity regulation or substituted the pooling process with a strided convolutional. These CNNs were implemented in end-to-end manner for classification, with extra Fully Connected and classification layer introduced to adjust them for COVID 19 infected categorization based on X-rays. According to the standard metrics accuracy, MCC and F-score, Table 4 reveals that the suggested 2 new novel CVD-HNet1 and CVD-HNet2 architectures could better distinguish the COVID 19 abnormalities from datasets.

Table 4 Proposed CVD-HNets versus Existing CNNs

Deep models	Accuracy	Sensitivity	Specificity	TP	FP	FN	TN	MCC	F score
Inceptionv3	96.82	0.97	0.97	626	20	21	624	0.94	0.97
DenseNet201	96.51	0.97	0.96	627	26	19	618	0.94	0.98
Google net	95.59	0.96	0.96	641	30	29	640	0.94	0.96
Squeeze Net	95.99	0.96	0.96	629	25	27	618	0.94	0.96
Xception	96.29	0.97	0.96	626	27	21	620	0.94	0.97
Resnet50	96.52	0.96	0.96	630	23	22	620	0.95	0.96
CVD-HNet1	98.15	0.97	0.98	640	9	17	635	0.97	0.97
CVD-HNet2	98.85	0.99	0.98	645	8	7	645	0.97	0.99

4.2 The Proposed Technique's Transfer Learning Based Optimization

Transfer learning is used to train the planned CVD-HNet1 and CVD-HNet2 using the X-ray dataset. CNNs are parametric, and best performance necessitates high volume data, but training with lesser X-ray images may result in convergence issues [76]. When a large dataset is unavailable, Transfer learning can be a methodology that has demonstrated favourable outcomes for CNN architectures. It allows the weight space of previously trained models to be reused and minimises overfitting in highly specified algorithms by giving a better initial set of weights [77]. As a result, we routinely used the concept of Transfer learning in this approach to accomplish significant results. In this case, we used the parameter space of the pre-trained model to initialise the weights of the suggested CVD-HNets [78]. Similarly, we are using the same training technique for existing CNN models to ensure a fair comparison. These models have now been optimised with X-ray images by applying domain adaptation enabled Transfer learning to modify the ImageNet pre trained techniques for categorization of COVID 19 specific pneumonia for the dataset. [79].

4.3 Proposed Methodology

The entire dataset has been split into two separate groups, each having an 80:20 percent ratio for the train and test sets (70% of X-ray pictures of the chest are used for training, 10% for validation purpose, and 20% for testing purpose). The fivefold cross validation technique was used to optimise the architectures parameters. SGD was utilised as an optimizer with a momentum of 0.94 during CNN training. Here learning rate was fixed as 0.0001 as well as weight decay was set as 0.0005. The model has been trained over ten epochs. For smooth training, a mini batch training has been used with batch size of 15 photos per epoch. Softmax can be utilised as activation function for all deep CNNs, and they were all optimised for picture classification by minimising cross-entropy loss. For the machine learning based classification analysis, ADAM was applied [80–85]. MATLAB 2019b was used to run all of the simulations. For MATLAB simulations, a 2.90 GHz Dell 8th gen intel core-7500 processor as well as a Multi core Nvidia GTX 1060 Tesla has been used. The models were trained for around 12 h. On the Nvidia Tesla K80, one epoch took 30–60 min to train. Figure 7. Provides the Performance analysis of proposed CVD-HNet1 and CVD-HNet2 models with Existing CNNs.

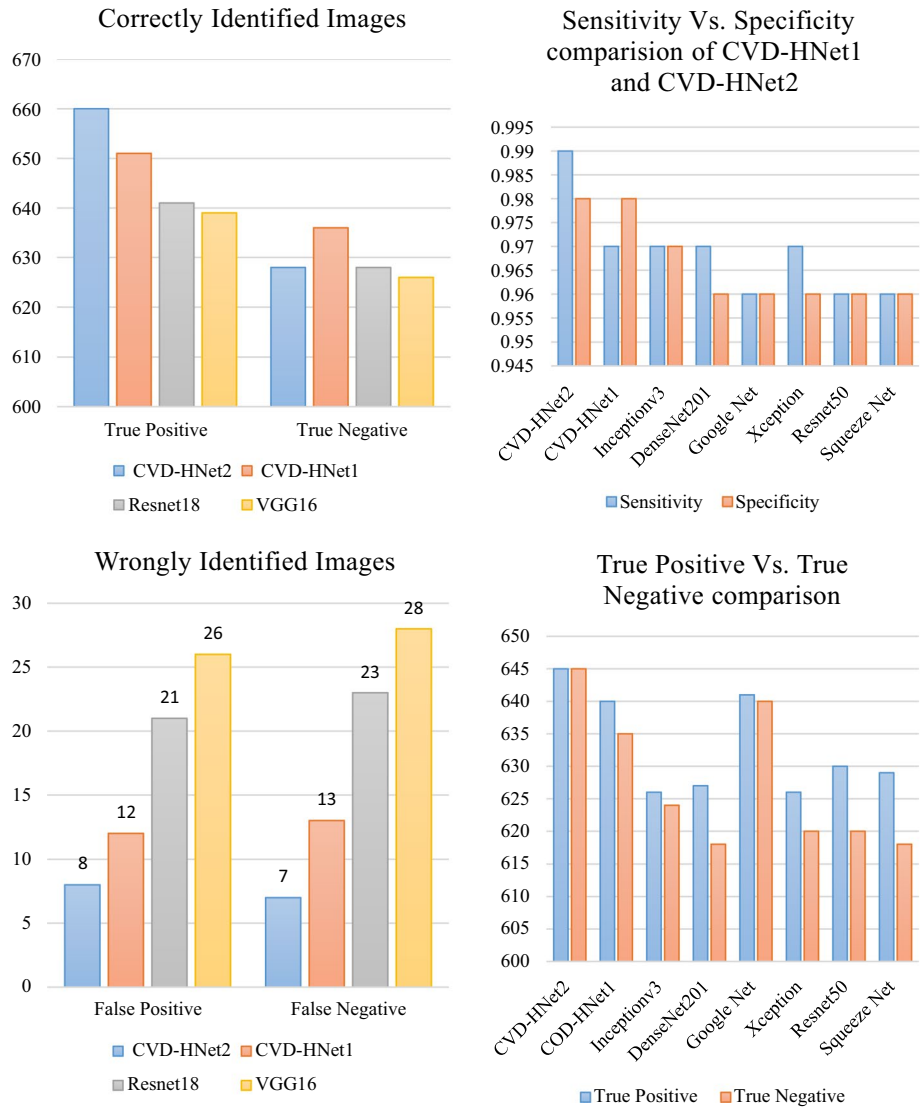

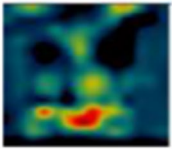
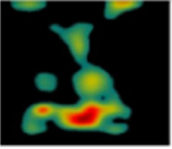

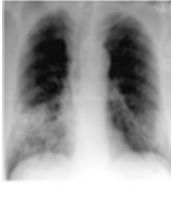
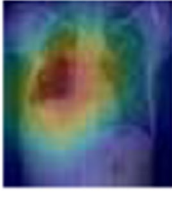
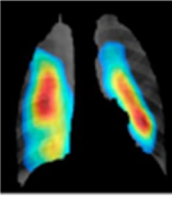


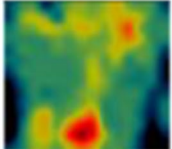
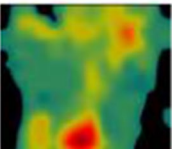

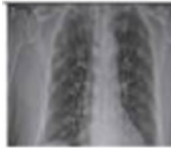
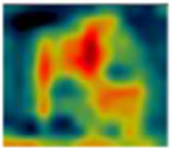
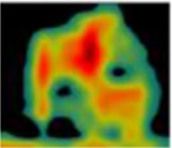
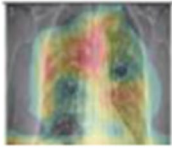


Fig. 7 Performance analysis of CVD-HNet1 and CVD-HNet2 with Existing CNNs

5 Results and Discussions

Utilizing chest X-ray images, this research describes a new novel deep CNN model for distinguishing COVID 19 affected cases. Two experiments have been carried out to empirically assess the efficiency of the suggested model. We looked at the benefits of synchronising employing max and average pooling in CVD-HNets for region classification in the first experiment shown in Table 5. The second section compares results to popular state-of-the-art methods in order to make a broad assessment of the COVID 19 identification challenge shown in Table 6.

Table 5 Correctly identified images

Classified image	Test image	Activation map	Segmented activation map	Composite image
Normal				
Bacterial pneumonia				
Viral pneumonia				
Covid 19 pneumonia				


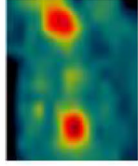
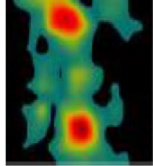


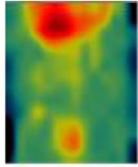
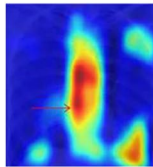


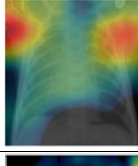
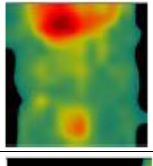


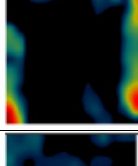
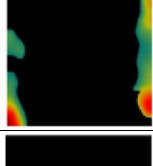


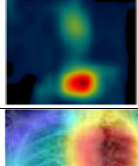
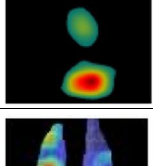
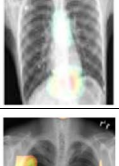
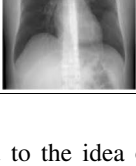

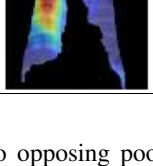
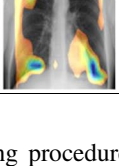
5.1 Performance Analysis of the Proposed CVD-HNets

There are a variety of metrics that may be used to assess the effectiveness of categorization models, including accuracy, sensitivity, specificity, F-score, precision, confusion matrix. Table 7 provides a mathematical description of the various measurements [86–90].

Here suggested CVD-HNet1 and CVD-HNet2 models are assessed using Accuracy, Matthews Correlation Coefficient and F score, which are conventional measurements in medical image diagnosis systems, on an unknown test dataset. Unlike Accuracy, both F score and Matthews Correlation Coefficient give recall and precision equal weight. 642 images of COVID 19 and normal people were accurately identified using the suggested CVD-HNet1 model. Similarly, the suggested CVD-HNet2 functions admirably, properly categorizing 631 COVID 19 afflicted and 636 normal people. The detection rate for COVID-19 tends to enhance when the depth is increased. Misclassification is most likely caused by lighting variations, low contrast areas, and a complex regions of images. In order to increase generalisation and improve robustness to unseen images, we used multiple data augmentation procedures during training (Fig. 8).

Benchmarking the feasibility of the suggested model against ResNet and VGG is used to assess its efficiency. ResNet-18 and VGG 16, the two baseline methods, are about as deep as CVD-HNet1 and CVD-HNet2. VGG 16 model uses a unique sort of pooling operators, whereas ResNet 18 employs strided convolution operation instead of pooling down,

Table 6 Wrongly identified images

Classified image	Test image	Activation map	Segmented activation map	Composite image	Results
Normal					Predicted class: Covid 19 pneumonia Predicted score: 0.9132
					Predicted class: Bacterial pneumonia Predicted score: 0.9241
					Predicted class: Viral pneumonia Predicted score: 0.9129
Pneumonia					Predicted class: Normal Predicted score 0.7123
					Predicted class: Covid 19 Predicted score: 0.7255
					Predicted class: Normal Predicted score 0.7436

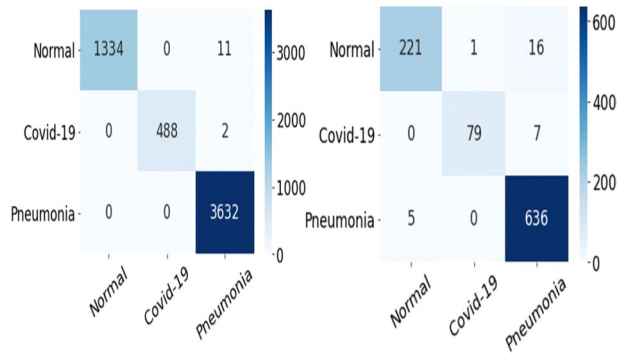
as opposed to the idea of employing two opposing pooling procedures in CVD-HNets. Table 2 shows the results comparison including Accuracy-98%, Matthews Correlation Coefficient -0.97 and F score-0.99 both CVD-HNets outperform ResNet 18 and VGG 16, according to performance analysis. In comparison to existing VGG16 and ResNet 18, the suggested CVD-HNets importantly enhance the metrics for both COVID 19 affected cases and healthy people.

In assessing the learning potential of deep CNN models, extracting feature is crucial. The contribution of the proposed model's feature set in learning class specified mappings is assessed using the traditional ML model. By extracting features from the proposed CVD-HNet's penultimate layer and allocating it to the ADAM classifier, mapping capacity of the suggested CVD-HNet is tested. Table 3 reveals that the sequence lent by proposed CVD-HNet1 and CVD-HNet2 can be used to distinguish COVID 19 cases from normal patients in two classes. Quantitative examination of Accuracy-98.84%,

Table 7 Performance matrices for classification

Sl. No	Metrics	Formula													
1	TP	If COVID-19 is identified in a COVID-19 affected person													
2	TN	If an individual is identified as NONCOVID-19 correctly													
3	FP	Depicts an inaccurate identification in which a healthy person is found to have COVID-19													
4	FN	Indicates an inaccurate identification in which a person affected with COVID-19 is mistakenly identified as a healthy person													
5	Accuracy	$\frac{\text{No. of Images Correctly predicted as both COVID - 19 and Non COVID}}{\text{Total No.of Images}}$ $= \frac{TP + TN}{(TP + TN + FP + FN)}$													
6	Sensitivity/Recall	$\frac{\text{No. of Images Correctly predicted as COVID-19}}{\text{Total No. of COVID-19 Images}} = \frac{TP}{(TP+FN)}$													
7	Specificity	$\frac{\text{No. of Images Correctly predicted as Non COVID-19}}{\text{Total No. of Non COVID-19 Images}} = \frac{TN}{(FN+FP)}$													
8	Precision	$\frac{\text{No. of Images Correctly predicted as COVID-19}}{\text{Total No. of predicted Positive Images}} = \frac{TP}{(TP+FP)}$													
9	F-Measure	$2 \times \frac{\text{Recall} \times \text{Precision}}{\text{Recall} + \text{Precision}}$													
10	Confusion Matrix	<table border="1" style="margin-left: auto; margin-right: auto;"> <tr> <td colspan="2" rowspan="2"></td> <th colspan="2">Predicted Class</th> </tr> <tr> <th>True Positive (TP)</th> <th>False Negative (FN)</th> </tr> <tr> <th rowspan="2">Actual Class</th> <th>True Positive (TP)</th> <td style="background-color: #d9ead3;">True Positive (TP)</td> <td style="background-color: #f4cccc;">False Negative (FN)</td> </tr> <tr> <th>False Positive (FP)</th> <td style="background-color: #f4cccc;">False Positive (FP)</td> <td style="background-color: #d9ead3;">True Negative (TN)</td> </tr> </table>			Predicted Class		True Positive (TP)	False Negative (FN)	Actual Class	True Positive (TP)	True Positive (TP)	False Negative (FN)	False Positive (FP)	False Positive (FP)	True Negative (TN)
		Predicted Class													
		True Positive (TP)	False Negative (FN)												
Actual Class	True Positive (TP)	True Positive (TP)	False Negative (FN)												
	False Positive (FP)	False Positive (FP)	True Negative (TN)												

Fig. 8 Confusion matrix



Matthews Correlation Coefficient-0.98, F score -0.99, and suggests that this technique outperforms ResNet 18 (Accuracy-96.64%, Matthews Correlation Coefficient-0.96, F score-0.97) and VGG-16 (Accuracy-95.90%, Matthews Correlation Coefficient -0.95, F score-0.96).

For a thorough empirical evaluation, we compared the proposed technique to popular CNN architectures on unseen chest X-ray pictures. Accuracy, MCC, AUC-ROC, F-score, precision and sensitivity used to evaluate the outcomes.

5.1.1 Performance Comparison with Existing CNNs

The suggested CVD-HNet1 and CVD-HNet2 are compared to DenseNet-201, GoogleNet, ResNet-50, InceptionV3, Xception, SqueezeNet, and in terms of performance [91–100]. In accordance with the standard performance metrics Accuracy, MCC, F score, and the performance analysis demonstrates that suggested CNN designs CVD-HNet1 and CVD-HNet2 could better distinguish the COVID 19 unique pneumonia affected regions from X-ray pictures. This increase the speed due to the proposed CNN architecture's systematic usage of max and average pooling operations.

6 Challenges and Future Directions

On ImageNet Challenger, the most important picture classification and segmentation challenge in the image analysis field, a considerable result was achieved using the numerous CNN-based deep neural networks constructed. The primary benefit of CNN over its counterparts is that it could detect critical properties without human assistance [101]. Table 6 shows how several classification models produced various performance indicators such as Accuracy, Sensitivity/Recall, Precision, Specificity, Receiver Operating Characteristic (ROC) Curves and F-measure. We may evaluate the best CNN model according to these performance metrics [102].

In recent days we've seen so much about imbalanced datasets, lack of confidence intervals [103], and also improperly labelled data in deep learning-related Medical Imaging literature which it is simple to label it the core obstacle while fully investigating Deep Learning (DL) breakthroughs [104–110]. The number of image samples and cases in database searches now available for diagnostic imaging activities is limited, with the exception of a few datasets. When compared with datasets for basic Computer Vision challenges that typically ranges from some few thousand to millions of labelled images [111], medical imaging datasets are far too small. Alternatively, now we are seeing a rising trend in the community of medical imaging professionals to learn deep models end-to-end, similar to what we're seeing in the wider Pattern Recognition community. Alternatively, the wider community has traditionally supported as such endeavours because large-scale labelled datasets are a required condition for producing correct DL models [112]. As an outcome, its unknown how well end-to-end certified DL models can execute medical image diagnosis activities without overfitting to training examples. Principal Component Analysis (PCA), Image flipping, image cropping, padding, and adversarial training are some of the basic data augmentation techniques we've created. These techniques, however, aren't as sophisticated as the Generative Adversarial Network when it comes to augmenting dataset images [113–115].

A further big stumbling block would be the usage of black boxes, the legitimate implications of black box functionality would be a disincentive, as Medicare practitioners could not trust on it. If the decision was unfavourable, who may be held liable? The hospital may be hesitant to utilise a black-box technique which could allow hospital to track that a certain outcome came from an optometrist, owed to the sensitivity of this location [116]. The black-box problem is an important research topic, and deep learning researchers are striving to address it [117].

Furthermore, teaching deep learning models is a very expensive endeavour due to the complicated data structures. They frequently demand high-end GPUs and hundreds of computers, raising the cost to users [118].

Because the increased complexity of numerous layers needs a large computing burden, training performance degrades as a result. To fight vanishing gradient and over-fitting concerns, researchers have used improved activation functions, drop-out techniques and cost function design [119]. High computational load has been addressed with the use of massively parallel technologies like GPU's and batch normalization [120]. The construction of an interdisciplinary data repository is made possible by the presence of a huge volume of electronic healthcare data.

7 Conclusion

Medical image diagnosis is a vital technology which bridges the gap between scientific and societal needs, and it has the potential to produce a substantial synergy that will benefit each of these sectors. Our investigation revealed the current state-of-the-art, which may be valuable to radiologists all over the world, according to the latest 120 medical imaging research papers. In this research, two new customized deep CNN methods are proposed to distinguish COVID 19 infected pneumonia cases from healthy people in X-ray pictures. The proposed COVID 19 classification method is compared against existing CNN models to see how well it performs. The proposed CVD-HNet1 and CVD-HNet2 models outperform existing CNN models and baseline in terms of Accuracy, MCC and F score according to experimental results. The proposed method is intended to aid physicians in the analysis of COVID 19 affected individuals. Furthermore, it provides a great potentiality in analysing various sorts of chest X-ray image anomalies. We discussed the current obstacles, main issues, and future directions.

Author Contributions All authors contributed to the study conception and design. Material preparation, data collection and analysis were performed by S.Suganyadevi, Dr.V.Seethalakshmi. The first draft of the manuscript was written by S.Suganyadevi and all authors commented on previous versions of the manuscript. All authors read and approved the final manuscript.

Funding No funding was received to assist with the preparation of this manuscript.

Availability of Data and Material The datasets generated during and/or analysed during the current study are available from the corresponding author on reasonable request.

Code Availability The code generated during and/or analysed during the current study are available from the corresponding author on reasonable request.

Declarations

Conflicts of interest The authors have no competing interests to declare that are relevant to the content of this article.

References

1. Wang, S., Zha, Y., Li, W., Wu, Q., Li, X., Niu, M., Wang, M., Qiu, X., Li, H., Yu, H., et al. (2020). A fully automatic deep learning system for COVID-19 diagnostic and prognostic analysis. *European Respiratory Journal*, 56(2), 2000775. <https://doi.org/10.1183/13993003.00775-2020>

2. Chen, J., Wu, L., Zhang, J., Zhang, L., Gong, D., Zhao, Y., Hu, S., Wang, Y., Hu, X., Zheng, B., et al. (2020). Deep learning-based model for detecting 2019 novel coronavirus pneumonia on high-resolution computed tomography. *Scientific Reports*, *10*, 19196. <https://doi.org/10.1038/s41598-020-76282-0>
3. Shi, F., Xia, L., Shan, F., Wu, D., Wei, Y., Yuan, H., Jiang, H., Gao, Y., Sui, H., & Shen D. (2020). Large-scale screening of COVID-19 from community acquired pneumonia using infection size-aware classification. Preprint <http://arxiv.org/abs/2003.09860>
4. Zheng, C., Deng, X., Fu, Q., Zhou, Q., Feng, J., Ma, H., Liu, W., & Wang, X. (2020). Deep learning-based detection for COVID-19 from chest CT using weak label. *MedRxiv*. <https://doi.org/10.1101/2020.03.12.20027185>
5. Fu, M., Yi, S.-L., Zeng, Y., Ye, F., Li, Y., Dong, X., Ren, Y.-D., Luo, L., Pan, J.-S., & Zhang, Q. (2020). Deep learning-based recognizing COVID-19 and other common infectious diseases of the lung by chest CT scan images. *MedRxiv*. <https://doi.org/10.1101/2020.03.28.20046045>
6. Maghddid, H. S., Asaad, A. T., Ghafoor, K. Z., Sadiq, A. S., & Khan, M. K. (2020). Diagnosing COVID-19 pneumonia from x-ray and CT images using deep learning and transfer learning algorithms. Preprint <http://arxiv.org/abs/2004.00038>
7. Ozkaya, U., Ozturk, S., & Barstugan, M. (2020). Coronavirus (COVID-19) classification using deep features fusion and ranking technique. Preprint <http://arxiv.org/abs/2004.03698>
8. Hu, S., Gao, Y., Niu, Z., Jiang, Y., Li, L., Xiao, X., Wang, M., Fang, E. F., MenpesSmith, W., Xia, J., et al. (2020). Weakly supervised deep learning for COVID-19 infection detection and classification from CT images. *IEEE Access*, *8*, 118,869–118,883.
9. Al-Karawi, D., Al-Zaidi, S., Polus, N., & Jassim, S. (2020). Machine learning analysis of chest CT scan images as a complementary digital test of coronavirus (COVID-19) patients. *MedRxiv*. <https://doi.org/10.1101/2020.04.13.20063479>
10. Amyar, A., Modzelewski, R., & Ruan, S. (2020). Multi-task deep learning based CT imaging analysis for COVID-19: Classification and segmentation. *MedRxiv*. <https://doi.org/10.1101/2020.04.16.20064709>
11. Wang, S., Kang, B., Ma, J., Zeng, X., Xiao, M., Guo, J., Cai, M., Yang, J., Li, Y., Meng, X., et al. (2020). A deep learning algorithm using CT images to screen for corona virus disease (COVID-19). *European Radiology*, *31*(8), 6096–6104. <https://doi.org/10.1007/s00330-021-07715-1>
12. Polsinelli, M., Cinque, L., & Placidi, G. (2020). A light cnn for detecting COVID-19 from CT scans of the chest. Preprint <http://arxiv.org/abs/2004.12837>.
13. Sun, L., Mo, Z., Yan, F., Xia, L., Shan, F., Ding, Z., Shao, W., Shi, F., Yuan, H., Jiang, H. et al. (2020). Adaptive feature selection guided deep forest for COVID-19 classification with chest CT. Preprint <http://arxiv.org/abs/2005.03264>.
14. Ahuja, S., Panigrahi, B. K., Dey, N., Rajinikanth, V., & Gandhi, T. K. (2020). Deep transfer learning-based automated detection of COVID-19 from lung CT scan slices. *Applied intelligence (Dordrecht, Netherlands)*, 1–15. <https://doi.org/10.1007/s10489-020-01826-w>
15. Hemdan, E. E.-D., Shouman, M. A., & Karar, M. E. (2020). COVIDx-net: A framework of deep learning classifiers to diagnose COVID-19 in x-ray images. Preprint <http://arxiv.org/abs/2003.11055>.
16. Narin, A., Kaya, C., & Pamuk, Z. (2020). Automatic detection of coronavirus disease (COVID-19) using x-ray images and deep convolutional neural networks. Preprint <http://arxiv.org/abs/2003.10849>.
17. Apostolopoulos, I. D., & Mpesiana, T. A. (2020). COVID-19: automatic detection from X-ray images utilizing transfer learning with convolutional neural networks. *Physical and Engineering Sciences in Medicine*, *43*, 635–640. <https://doi.org/10.1007/s13246-020-00865-4>
18. Hassanien, A. E., Mahdy, L. N., Ezzat, K. A., Elmousalami, H. H., & Ella, H. A. (2020). Automatic X-ray COVID-19 lung image classification system based on multi-level thresholding and support vector machine. *MedRxiv*. <https://doi.org/10.1101/2020.03.30.20047787>
19. Maghddid, H. S., Asaad, A. T., Ghafoor, K. Z., Sadiq, A. S., & Khan, M. K. (2020). Diagnosing COVID-19 pneumonia from x-ray and CT images using deep learning and transfer learning algorithms. Preprint <http://arxiv.org/abs/2004.00038>.
20. Farooq, M., & Hafeez, A. (2020). COVID-resnet: A deep learning framework for screening of COVID19 from radiographs. Preprint <http://arxiv.org/abs/2003.14395>.
21. Apostolopoulos, I. D., Aznaouridis, S. I., & Tzani, M. A. (2020). Extracting possibly representative COVID-19 biomarkers from X-ray images with deep learning approach and image data related to pulmonary diseases. *Journal of Medical and Biological Engineering*, *40*, 462–469. <https://doi.org/10.1007/s40846-020-00529-4>
22. Khalifa, N. E. M., Taha, M. H. N., Hassanien, A. E., & Elghamrawy, S. (2020). Detection of coronavirus (COVID-19) associated pneumonia based on generative adversarial networks and a re-tuned deep transfer learning model using chest X-ray dataset. Preprint <http://arxiv.org/abs/2004.01184>.

23. Karim, M., Dohmen, T., Rebholz-Schuhmann, D., Decker, S., Cochez, M., Beyan, O. et al. (2020). \DeepCOVIDexplainer: Explainable COVID-19 predictions based on chest X-ray images. Preprint <http://arxiv.org/abs/2004.04582>.
24. Khan, A. I., Shah, J. L., & Bhat, M. M. (2020). Coronet: A deep neural network for detection and diagnosis of COVID-19 from chest X-ray images. *Computer Methods and Programs in Biomedicine*, 196, 105581. <https://doi.org/10.1016/j.cmpb.2020.105581>
25. Afshar, P., Heidarian, S., Naderkhani, F., Oikonomou, A., Plataniotis, K. N., & Mohammadi, A. (2020). COVID-caps: A capsule network-based framework for identification of COVID-19 cases from X-ray images. Preprint <http://arxiv.org/abs/2004.02696>.
26. Minaee, S., Kaeh R., Sonka, M., Yazdani, S., & Sou, G. J. (2020). Deep-COVID: Predicting COVID-19 from chest X-ray images using deep transfer learning. Preprint <http://arxiv.org/abs/2004.09363>.
27. Sethy, P. K., & Behera, S. K. (2020). \Detection of coronavirus disease (COVID-19) based on deep features. *Preprints, 2020030300*, 2020.
28. Zhang, Y., Niu, S., Qiu, Z., Wei, Y., Zhao, P., Yao, J., Huang, J., Wu, Q. and Tan, M. (2020). \COVID-da: Deep domain adaptation from typical pneumonia to COVID-19. Preprint <http://arxiv.org/abs/2005.01577>.
29. Oh, Y., Park, S., & Ye, J. C. (2020). Deep learning COVID-19 features on CXR using limited training data sets. *IEEE Transactions on Medical Imaging*, 39(8), 2688–2700. <https://doi.org/10.1109/TMI.2020.2993291>
30. Yamac, M., Ahishali, M., Degerli, A., Kiranyaz, S., Chowdhury, M. E., & Gabbouj, M. (2020). Convolutional sparse support estimator based COVID-19 recognition from X-ray images. Preprint <http://arxiv.org/abs/2005.04014>.
31. Wang, L., & Wong, A. (2020). COVID-net: A tailored deep convolutional neural network design for detection of COVID-19 cases from chest X-ray images. Preprint <http://arxiv.org/abs/2003.09871>.
32. Ahishali, M., Degerli, A., Yamac, M., Kiranyaz, S., Chowdhury, M. E., Hameed, K., Hamid, T., Mazhar, R., & Gabbouj, M. (2020). A comparative study on early detection of COVID-19 from chest X-ray images. Preprint <http://arxiv.org/abs/2006.05332>.
33. Abbas, A., Abdelsamea, M. M., & Gaber, M. (2020). 4s-dt: Self supervised super sample decomposition for transfer learning with application to COVID-19 detection. Preprint <http://arxiv.org/abs/2007.11450>.
34. Boudrioua, M. S. (2020). COVID-19 detection from chest X-ray images using cnns models: Further evidence from deep transfer learning. Available at SSRN 3630150.
35. Manapure, P., Likhari, K., & Kosare, H. (2020). Detecting COVID-19 in X-ray images with keras, tensor flow, and deep learning. *International Journal of Computer Science Trends and Technology (IJCTST)*, 2(3).
36. Al-antari, M. A., Hua, C.-H., & Lee, S. (2020). Fast deep learning computer-aided diagnosis against the novel COVID-19 pandemic from digital chest X-ray images. <https://doi.org/10.21203/rs.3.rs-36353/v1>
37. Brunese, L., Mercaldo, F., Reginelli, A., & Santone, A. (2020). Explainable deep learning for pulmonary disease and coronavirus COVID-19 detection from X-rays. *Computer Methods and Programs in Biomedicine*, 196, 105608. <https://doi.org/10.1016/j.cmpb.2020.105608>
38. Salih, S. Q., Abdulla, H. K., Ahmed, Z. S., Surameery, N. M. S., & Rashid, R. D. (2020). Modified alexnet convolution neural network for COVID-19 detection using chest X-ray images. *Kurdistan Journal of Applied Research*, 119–130.
39. Chatterjee, S., Saad, F., Sarasaen, C., Ghosh, S., Khatun, R., Radeva, P., Rose, G., Stober, S., Speck, O., & Nu'rnberger, A. (2020). Exploration of interpretability techniques for deep COVID-19 classification using chest X-ray images. Preprint <http://arxiv.org/abs/2006.02570>.
40. Khan, S. H., Sohail, A., Zafar, M. M., & Khan, A. (2021). Coronavirus disease analysis using chest X-ray images and a novel deep convolutional neural network. *Photodiagnosis and Photodynamic Therapy*, 35, 102473. <https://doi.org/10.1016/j.pdpdt.2021.102473>
41. Liang, S., Liu, H., Gu, Y., et al. (2021). Fast automated detection of COVID-19 from medical images using convolutional neural networks. *Commun Biol*, 4, 35. <https://doi.org/10.1038/s42003-020-01535-7>
42. Dong, D., Tang, Z., Wang, S., Hui, H., Gong, L., Lu, Y., Xue, Z., Liao, H., Chen, F., Yang, F., Jin, R., Wang, K., Liu, Z., Wei, J., Mu, W., Zhang, H., Jiang, J., Tian, J., & Li, H. (2021). The Role of Imaging in the Detection and Management of COVID-19: A Review. *IEEE reviews in biomedical engineering*, 14, 16–29. <https://doi.org/10.1109/RBME.2020.2990959>
43. Vasilev, Y. A., Sergunova, K. A., Bazhin, A. V., Masri, A. G., Vasileva, Y. N., Semenov, D. S., Kudryavtsev, N. D., Panina, O. Y., Khoruzhaya, A. N., Zinchenko, V. V., Akhmad, E. S., Petraikin,

- A. V., Vladzmyrskyy, A. V., Midaev, A. V., & Morozov, S. P. (2021). Chest MRI of patients with COVID-19. *Magnetic resonance imaging*, 79, 13–19. <https://doi.org/10.1016/j.mri.2021.03.005>
44. Torkiana, P., Rajebib, H., Zamanic, T., Ramezanid, N., Kianid, P., & Akhlaghpood, S. (2021). Magnetic resonance imaging features of coronavirus disease 2019 (COVID19) pneumonia: The first preliminary case series'. *Clinical Imaging*, 69, 261–265. <https://doi.org/10.1016/j.clinimag.2020.09.002>
 45. Ojha, V.*, Verma, M.*, Pandey, NN.*, Mani, A.†, Malhi A. S.*, Kumar, S.*, Jagia, P.*, Roy, A.‡, Sharma, S.* (2021). Cardiac magnetic resonance imaging in coronavirus disease 2019 (COVID-19), *Journal of Thoracic Imaging*, 36(2), 73–83. <https://doi.org/10.1097/RTI.0000000000000574>.
 46. Ates, O. F., Taydas, O., & Dheir, H. (2020). Thorax magnetic resonance imaging findings in patients with coronavirus disease (COVID-19). *Academicradiology*, 27(10), 373–1378. <https://doi.org/10.1016/j.acra.2020.08.009>.
 47. Reshi, A. A., Rustam, F., Mehmood, A., Alhossan, A., Alrabiah, Z., Ahmad, A., Alsuwailam, H., & Choi, G. S. (2021). An efficient CNN model for COVID-19 disease detection based on X-ray image classification". *Complexity*, 2021(6621607), 12. <https://doi.org/10.1155/2021/6621607>
 48. Das, A. K., Ghosh, S., Thunder, S., et al. (2021). Automatic COVID-19 detection from X-ray images using ensemble learning with convolutional neural network. *Pattern Analysis and Applications*, 24, 1111–1124. <https://doi.org/10.1007/s10044-021-00970-4>
 49. Albahli, S., & Yar, G. (2021). Fast and accurate detection of COVID-19 along with 14 other chest pathologies using a multi-level classification: Algorithm development and validation study. *Journal of Medical Internet Research*, 23(2), e23693.
 50. Sarki, R., Ahmed, K., Wang, H., Zhang, Y., Wang, K. Automated Detection of COVID-19 through Convolutional Neural Network using Chest X-ray images. medRxiv 2021.02.06.21251271. <https://doi.org/10.1101/2021.02.06.21251271>.
 51. Chakravorti, T., Addala, V. K. and Verma, J. S. (2021) Detection and classification of COVID 19 using convolutional neural network from chest X-ray images. In: 2021 6th international conference for convergence in technology (I2CT), pp. 1–6. <https://doi.org/10.1109/I2CT51068.2021.9418221>.
 52. Agrawal, T., & Choudhary, P. (2021). FocusCOVID: Automated COVID-19 detection using deep learning with chest X-ray images. *Evolving Systems*. <https://doi.org/10.1007/s12530-021-09385-2>
 53. Roberts, M., Driggs, D., Thorpe, M., et al. (2021). Common pitfalls and recommendations for using machine learning to detect and prognosticate for COVID-19 using chest radiographs and CT scans. *Nat Mach Intell*, 3, 199–217. <https://doi.org/10.1038/s42256-021-00307-0>
 54. Silva, P., Luz, E., Silva, G., Moreira, G., Silva, R., Lucio, D., & Menotti, D. (2020). COVID-19 detection in CT images with deep learning: A voting-based scheme and cross-datasets analysis. *Informatics in Medicine Unlocked*, 20, 100427. <https://doi.org/10.1016/j.imu.2020.100427>
 55. Perumal, V., Narayanan, V. and Rajasekar, S.J.S. (2021) Prediction of COVID-19 with Computed Tomography Images using Hybrid Learning Techniques. Imaging Disease Markers as a Diagnostic, Prognostic, and Educational Tool, 2021(5522729). <https://doi.org/10.1155/2021/5522729>
 56. Hosny, K. M., Darwish, M. M., Li, K., & Salah, A. (2021). COVID-19 diagnosis from CT scans and chest X-ray images using low-cost Raspberry Pi. *PLoS ONE*, 16(5), e0250688. <https://doi.org/10.1371/journal.pone.0250688>
 57. Mishra, A. K., Das, S. K., Roy, P. and Bandyopadhyay, S. Identifying COVID19 from chest CT images: A deep convolutional neural networks based approach. 2020(8843664). <https://doi.org/10.1155/2020/8843664>
 58. Shah, V., Keniya, R., Shridharani, A., et al. (2021). Diagnosis of COVID-19 using CT scan images and deep learning techniques. *Emergency Radiology*, 28, 497–505. <https://doi.org/10.1007/s10140-020-01886-y>
 59. Halder, A., & Datta, B. (2021). COVID-19 detection from lung CT-scan images using transfer learning approach. *Machine Learning: Science and Technology*, 2, 045013. <https://doi.org/10.1088/2632-2153/abf22c>
 60. James, R. M. and Sunyoto, A. (2020) Detection Of CT - scan lungs COVID-19 image using convolutional neural network and CLAHE. In 2020 3rd international conference on information and communications technology (ICOIACT), pp. 302–307. <https://doi.org/10.1109/ICOIACT50329.2020.9332069>.
 61. Elaziz, M. A., Hosny, K. M., Salah, A., Darwish, M. M., Lu, S., & Sahlol, A. T. (2020). New machine learning method for image-based diagnosis of COVID-19. *PLoS ONE*, 15(6), e0235187.
 62. Mei, X., Lee, H. C., Diao, K., et al. (2020). Artificial intelligence-enabled rapid diagnosis of patients with COVID-19. *Nature Medicine*, 26, 1224–1228. <https://doi.org/10.1038/s41591-020-0931-3>
 63. Birenbaum, A., Greenspan, H. (2016) Longitudinal multiple sclerosis lesion segmentation using multi-view convolutional neural networks. In *Proceedings of the Deep Learning in Medical Image*

- Analysis (DLMIA)*. Lecture Notes in Computer Science, 10 0 08, pp. 58–67. https://doi.org/10.1007/978-3-319-46976-8_7
64. Cheng, X., Zhang, L., & Zheng, Y. (2015). Deep similarity learning for multimodal medical images. *Computer Methods in Biomechanics and Biomedical Engineering*. <https://doi.org/10.1080/21681163.2015.1135299>
 65. Cicero, M., Bilbily, A., Colak, E., Dowdell, T., Gray, B., Perampaladas, K., & Barfett, J. (2017). Training and validating a deep convolutional neural network for computer-aided detection and classification of abnormalities on frontal chest radiographs. *Investigative Radiology*, 52(5), 281–287. <https://doi.org/10.1097/RLI.0000000000000341>
 66. Ertosun, M. G., Rubin, D. L. Automated Grading of Gliomas using Deep Learning in Digital Pathology Images: A modular approach with ensemble of convolutional neural networks. In *AMIA Annual Symposium Proceedings*. 2015 Nov 5; 2015:1899–908.PMID: 26958289; PMCID: PMC4765616.
 67. Guo, Y., Gao, Y., & Shen, D. (2016). Deformable MR prostate segmentation via deep feature learning and sparse patch matching. *IEEE Transactions on Medical Imaging*, 35(4), 1077–1089. <https://doi.org/10.1109/TMI.2015.2508280>
 68. Guo, Y., Wu, G., Commander, L. A., Szary, S, Jewells, V, Lin, W., Shen, D. (2014) Segmenting hippocampus from infant brains by sparse patch matching with deep-learned features. In *Proceedings of the Medical Image Computing and Computer-Assisted Intervention*. Lecture Notes in Computer Science, Vol. 8674, pp. 308–315. https://doi.org/10.1007/978-3-319-10470-6_9
 69. Han, X. H., Lei, J., Chen, Y. W. (2016) HEP-2 cell classification using K -support spatial pooling in deep CNNs. In *Proceedings of the deep learning in medical image analysis (DLMIA)*. Lecture notes in computer science, 10 0 08, pp 3–11. https://doi.org/10.1007/978-3-319-46976-8_1
 70. Haugeland, J. (1985). *Artificial Intelligence: The Very Idea*. The MIT Press.
 71. Havaei, M., Davy, A., Warde Farley, D., Biard, A., Courville, A., Bengio, Y., Pal, C., Jodoin, P. M., & Larochelle, H. (2016). Brain tumor segmentation with deep neural networks. *Medical Image Analysis*, 35, 18–31. <https://doi.org/10.1016/j.media.2016.05.004>
 72. Havaei, M., Guizard, N., Chapados, N., Bengio, Y. (2016) HeMIS: Hetero-modal image segmentation. In: *Proceedings of the medical image computing and computer-assisted intervention*. In: Lecture Notes in Computer Science, 9901, pp 469–477. https://doi.org/10.1007/978-3-319-46723-8_54
 73. He K, Zhang X, Ren S, Sun J. (2015) Deep residual learning for image recognition. Preprint <http://arxiv.org/abs/1512.03385>.
 74. Janowczyk, A., & Madabhushi, A. (2016). Deep learning for digital pathology image analysis: a comprehensive tutorial with selected use cases. *Journal of Pathology Informatics*, 7, 29. <https://doi.org/10.4103/2153-3539.186902>
 75. Jia, Y., Shelhamer, E., Donahue, J., Karayev, S., Long, J., Girshick, R., Guadarrama, S. and Darrell, T. (2014) Caffe: Convolutional architecture for fast feature embedding. In *Proceedings of the Twenty-Second ACM International Conference on Multi-media*, pp. 675–678. <https://doi.org/10.1145/2647868.2654889>
 76. Kainz P, Pfeiffer M, Urschler M. (2015) Semantic segmentation of colon glands with deep convolutional neural networks and total variation segmentation. Preprint <http://arxiv.org/abs/1511.06919>.
 77. Kallen, H., Molin, J., Heyden, A., Lundstr, C., Astrom, K. (2016) Towards grading gleason score using generically trained deep convolutional neural networks. In *Proceedings of the IEEE International Symposium on Biomedical Imaging*, pp. 1163–1167. <https://doi.org/10.1109/ISBI.2016.7493473>
 78. Balasamy, K., & Suganyadevi, S. (2021). A fuzzy based ROI selection for encryption and watermarking in medical image using DWT and SVD. *Multimedia Tools Applications*, 80, 7167–7186. <https://doi.org/10.1007/s11042-020-09981-5>
 79. Lekadir, K., Galimzianova, A., Betriu, A., Del Mar, V. M., Igual, L., Rubin, D. L., Fernandez, E., Radeva, P., & Napel, S. (2017). A convolutional neural network for automatic characterization of plaque composition in carotid ultrasound. *IEEE Journal of Biomedical Health Informatics.*, 21, 48–55. <https://doi.org/10.1109/JBHI.2016.2631401>
 80. Li, R., Zhang, W., Suk, H. I., Wang, L., Li, J., Shen, D., & Ji, S. (2014). Deep learning based imaging data completion for improved brain disease diagnosis. *Medical Image Computing and Computer Assisted Intervention*, 17(Pt 3), 305–312. https://doi.org/10.1007/978-3-319-0443-0_39
 81. Balasamy, K., Krishnaraj, N., & Vijayalakshmi, K. (2021). An adaptive neuro-fuzzy based region selection and authenticating medical image through watermarking for secure communication. *Springer - Wireless Personal Communications*. [https://doi.org/10.1007/s11277-021-09031-9.\(IF-1.671\)](https://doi.org/10.1007/s11277-021-09031-9.(IF-1.671))

82. Miao, S., Wang, Z. J., & Liao, R. (2016). A CNN regression approach for real-time 2D/3D registration. *IEEE Transactions on Medical Imaging*, 35(5), 1352–1363. <https://doi.org/10.1109/TMI.2016.2521800>
83. Moeskops, P., Viergever, M. A., Mendrik, A. M., de Vries, L. S., Benders, M. J. N. L., & Išgum, I. (2016). Automatic segmentation of MR brain images with a convolutional neural network. *IEEE Transactions on Medical Imaging*, 35(5), 1252–1262. <https://doi.org/10.1109/TMI.2016.2548501>
84. Pinaya, W. H. L., Gadelha, A., Doyle, O. M., Noto, C., Zugman, A. C. Q., Jackowski, A. P., Bressan, R. A., & Sato, J. R. (2016). Using deep belief network modelling to characterize differences in brain morphometry in schizophrenia. *Nature Scientific Reports*, 6, 38897. <https://doi.org/10.1038/srep38897>
85. Plis, S. M., Hjelm, D. R., Salakhutdinov, R., Allen, E. A., Bockholt, H. J., Long, J. D., Johnson, H. J., Paulsen, J. S., Turner, J. A., & Calhoun, V. D. (2014). Deep learning for neuroimaging: a validation study. *Frontiers in Neuroscience*. <https://doi.org/10.3389/fnins.2014.00229>
86. Poudel, R. P. K., Lamata, P., Montana, G. (2016) Recurrent fully convolutional neural networks for multi-slice MRI cardiac segmentation. Preprint <http://arxiv.org/abs/1608.03974>.
87. Suganyadevi, S., Seethalakshmi, V., & Balasamy, K. (2021). A review on deep learning in medical image analysis. *International Journal of Multimedia Information Retrieval*. <https://doi.org/10.1007/s13735-021-00218-1>
88. Rajkomar, A., Lingam, S., Taylor, A. G., Blum, M., & Mongan, J. (2017). High-throughput classification of radiographs using deep convolutional neural networks. *Journal of Digital Imaging*, 30, 95–101. <https://doi.org/10.1007/s10278-016-9914-9>
89. Ravi, D., Wong, C., Deligianni, F., Berthelot, M., Andreu Perez, J., Lo, B., & Yang, G. Z. (2017). Deep learning for health informatics. *IEEE Journal Biomedical and Health Informatics*, 21, 4–21. <https://doi.org/10.1109/JBHI.2016.2636665>
90. Ravishankar, H., Prabhu, S. M., Vaidya, V., Singhal, N., (2016) Hybrid approach for automatic segmentation of fetal abdomen from ultrasound images using deep learning. In *Proceedings of the IEEE International Symposium on Biomedical Imaging*, pp. 779–782. <https://doi.org/10.1109/ISBI.2016.7493382>
91. Ramakrishnan, S., Gopalakrishnan, T., Balasamy, K. Svd based robust digital watermarking for still images using wavelet transform. CCSEA 2011, CS & IT 02.
92. Samala, R., Chan, H. P., Hadjiiski, L., Cha, K., & Helvie, M. (2016). Deep learning and transfer learning techniques based stacking approach for accurate Invasive Ductal Carcinoma classification using histology images. *Journal of Intelligent & Fuzzy Systems*, (Preprint), 1–12. <https://doi.org/10.1117/12.2217092>
93. Samala, R. K., Chan, H. P., Hadjiiski, L., Helvie, M. A., Wei, J., & Cha, K. (2016). Mass detection in digital breast tomosynthesis: Deep convolutional neural network with transfer learning from mammography. *Medical Physics*, 43(12), 6654. <https://doi.org/10.1118/1.4967345>
94. Sarraf, S., & Tofghi, G. (2016). Classification of Alzheimer's disease using fmri data and deep learning convolutional neural networks. Preprint <http://arxiv.org/abs/1603.08631>.
95. Schaumberg A.J, Rubin M.A, Fuchs T.J. (2016). H&E stained whole slide deep learning predicts SPOP mutation state in prostate cancer. Preprint <http://arxiv.org/abs/064279>. <https://doi.org/10.1101/064279>
96. Suganyadevi, S., Shamia, D., & Balasamy, K. (2021). An IoT-based diet monitoring healthcare system for women. *Smart Healthcare System Design: Security and Privacy Aspects*. <https://doi.org/10.1002/9781119792253.ch8>
97. Spampinato, C., Palazzo, S., Giordano, D., Aldinucci, M., Leonardi, R. (2016). Deep learning for automated skeletal bone age assessment in X-ray images. *Med Image Anal.* 2017 Feb;36: pp 41-51. <https://doi.org/10.1016/j.media.2016.10.029>. PMID: 2781686
98. Balasamy, K., & Shamia, D. (2021). Feature extraction-based medical image watermarking using fuzzy-based median filter. *IETE Journal of Research*. <https://doi.org/10.1080/03772063.2021.1893231>
99. Stern, D., Payer, C., Lepetit, V., Urschler, M. (2016). Automated age estimation from hand MRI volumes using deep learning. In *Proceedings of the medical image computing and computer-assisted intervention*. Lecture Notes in Computer Science, Vol. 9901, pp. 194–202. https://doi.org/10.1007/978-3-319-46723-8_23
100. Suk, H. I., & Shen, D. (2013). Deep learning based feature representation for AD/MCI classification. In *Proceedings of the medical image computing and computer-assisted intervention*. Lecture Notes in Computer Science, Vol. 8150, pp. 583–590. https://doi.org/10.1007/978-3-642-40763-5_72

101. Sun W, Tseng TB, Zhang J, Qian W. (2016). Enhancing deep convolutional neural network scheme for breast cancer diagnosis with unlabeled data. *Comput Med Imaging Graph.* 2017 Apr;57:4–9. <https://doi.org/10.1016/j.compmedimag>. Epub 2016 Jul 19. PMID: 27475279.
102. Balasamy, K., Krishnaraj, N., Ramprasath, J., Ramprakash, P., (2021). A secure framework for protecting clinical data in medical IoT environment. *Smart Healthcare System Design: Security and Privacy Aspects*, Wiley. <https://doi.org/10.1002/9781119792253.ch9>
103. Teikari, P., Santos, M., Poon, C., Hynynen, K. (2016). Deep learning convolutional networks for multiphoton microscopy vasculature segmentation. Preprint <http://arxiv.org/abs/1606.02382>.
104. Tran, P.V. (2016). A fully convolutional neural network for cardiac segmentation in short axis MRI. Preprint <http://arxiv.org/abs/1604.00494>.
105. Xie, Y., Xing, F., Kong, X., Su, H., Yang, L. (2015). Beyond classification: structured regression for robust cell detection using convolutional neural network. In *Proceedings of the Medical Image Computing and Computer-Assisted Intervention*. Lecture Notes in Computer Science, 9351, pp. 358–365. https://doi.org/10.1007/978-3-319-24574-4_43
106. Xie, Y., Zhang, Z., Sapkota, M., Yang, L. (2016). Spatial clockwork recurrent neural network for muscle perimysium segmentation. In *Proceedings of the International Conference on Medical Image Computing and Computer-Assisted Intervention*. Lecture Notes in Computer Science, 9901. Springer, pp. 185–193. https://doi.org/10.1007/978-3-319-46723-8_22
107. Xu, T., Zhang, H., Huang, X., Zhang, S., Metaxas, D. N. (2016). Multimodal deep learning for cervical dysplasia diagnosis. In *Proceedings of the Medical Image Computing and Computer-Assisted Intervention*. Lecture Notes in Computer Science, 9901, pp 115–123. https://doi.org/10.1007/978-3-319-46723-8_14
108. Krishnasamy, B., Balakrishnan, M., & Christopher, A. (2021). A genetic algorithm based medical image watermarking for improving robustness and fidelity in wavelet domain. In *Intelligent data engineering and analytics. Advances in Intelligent systems and computing*, Vol. 1177. Springer. https://doi.org/10.1007/978-981-15-679-1_27
109. Xu Z, Huang J. (2016). Detecting cells in one second. In *Proceedings of the Medical Image Computing and Computer-Assisted Intervention*. Lecture Notes in Computer Science, Vol. 9901, pp. 676–684. https://doi.org/10.1007/978-3-319-46723-8_78
110. Yang, D., Zhang, S., Yan, Z., Tan, C., Li, K., Metaxas, D. (2015). Automated anatomical landmark detection on distal femur surface using convolutional neural network. In *Proceedings of the IEEE International Symposium on Biomedical Imaging*, pp. 17–21. <https://doi.org/10.1109/isbi.2015.7163806>
111. Yang, H., Sun, J., Li, H., Wang, L., & Xu, Z. (2016). Deep fusion net for multi-atlas segmentation: Application to cardiac MR images. In *Proceedings of the medical image computing and computer assisted intervention*. Lecture Notes in Computer Science, Vol. 9901, pp 521–528. https://doi.org/10.1007/978-3-319-46723-8_60
112. Wang, S., Yao, J., Xu, Z., Huang, J. (2016). Subtype cell detection with an accelerated deep convolutional neural network. In *Proceedings of the medical image computing and computer-assisted intervention*. Lecture Notes in Computer Science, Vol. 9901, pp. 640–648. https://doi.org/10.1007/978-3-319-46723-8_74
113. Xu, Y., Mo, T., Feng, Q., Zhong, P., Lai, M. & Chang, E. I. C. (2014). Deep learning of feature representation with multiple instance learning for medical image analysis. In *Proceedings of the IEEE international conference on acoustics, speech and signal processing (ICASSP)*, pp. 1626–1630. <https://doi.org/10.1109/ICASSP.2014.6853873>
114. Yang, X., Kwitt, R., Niethammer, M. (2016). Fast predictive image registration. In *Proceedings of the Deep Learning in Medical Image Analysis (DLMIA)*. Lecture Notes in Computer Science, 10 0 08, pp. 48–57. https://doi.org/10.1007/978-3-319-46976-8_6
115. Yao, J., Wang, S., Zhu, X., & Huang, J. (2016). Imaging biomarker discovery for lung cancer survival prediction. In: *Proceedings of the medical image computing and computer-assisted intervention*. Lecture Notes in Computer Science, 9901, pp. 649–657. https://doi.org/10.1007/978-3-319-46723-8_75
116. Zhao, J., Zhang, M., Zhou, Z., Chu, J., & Cao, F. (2017). Automatic detection and classification of leukocytes using convolutional neural networks. *Medical & Biological Engineering & Computing*, 55(8), 1287–1301. <https://doi.org/10.1007/s11517-016-1590-x>
117. Zhang, Q., Xiao, Y., Dai, W., Suo, J., Wang, C., Shi, J., & Zheng, H. (2020). Deep learning based classification of breast tumors with shear-wave elastography. *Ultrasonics*, 72, 150–157. <https://doi.org/10.3389/fonc.2020.01621>

118. Zhang, H., Li, L., Qiao, K., Wang, L., Yan, B., Li, L., & Hu, G. (2016). Image prediction for limited-angle tomography via deep learning with convolutional neural network. Preprint <http://arxiv.org/abs/1607.08707>.
119. Zeiler, M. D. & Fergus, R. (2014). Visualizing and understanding convolutional networks. In *Proceedings of the European Conference on Computer Vision*, pp. 818–833.
120. Yu, L., Yang, X., Chen, H., Qin, J., Heng, & P.-A. (2017). Volumetric convnets with mixed residual connections for automated prostate segmentation from 3D MR images. In: *Proceedings of the thirty-first AAAI conference on artificial intelligence*, pp. 66–72.

Publisher's Note Springer Nature remains neutral with regard to jurisdictional claims in published maps and institutional affiliations.



S. Suganyadevi has done her B.E in Electronics and Communication Engineering with distinction from Erode Sengunthar Engineering College, Erode, Tamilnadu, M.E in VLSI Design from Bannari Amman Institute of Technology, Erode, Tamilnadu and currently doing Ph.D in Information and Communication Engineering from Anna University, Chennai. Her research interest is Signal Processing, Image Processing, Machine Learning, Medical Imaging, Low power VLSI Design, Internet of Things. She has 5 years experience in teaching.



V. Seethalakshmi has done her B.E in Electrical and Electronics Engineering with distinction from PSG college of Technology, Coimbatore, Tamilnadu, M.Tech in Electronics and Communication Engineering from PTU university, Punjab and Ph.D in Information and Communication Engineering from Anna University, Chennai. Her research interest is Wireless Communication, Wireless and Adhoc Networks. She has rich 23 years of experience in industry as well as teaching. She has published 28 technical papers in refereed journals, 49 research papers in national and International conferences and published 5 books and 3 patents. She is a recognized supervisor of Anna University, Chennai and 3 research scholars are pursuing PhD under her supervision. She is an active member of various professional societies like ISTE, IAENG, IACSIT, UACEE, CSTA and SDIWC. She is reviewer for 3 refereed journals and got certificate of outstanding contribution in reviewing by simulation modeling and practices, Elsevier Journal.